In Situ Stresses in Borehole Blanche-1/ South Australia Derived from Breakouts, Core Discing and Hydraulic Fracturing to 2 km Depth

G. Klee, A. Bunger, G. Meyer, F. Rummel & B. Shen

Rock Mechanics and Rock Engineering

ISSN 0723-2632
Volume 44
Number 5

Rock Mech Rock Eng (2011)
44:531-540
DOI 10.1007/s00603-011-0157-2

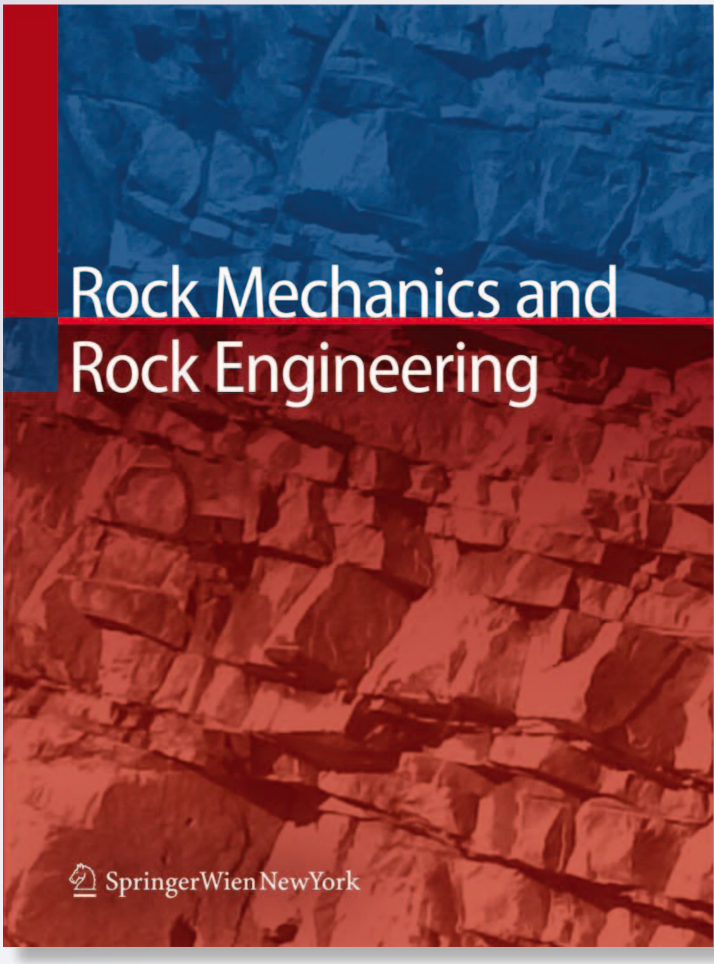

Rock Mech Rock Eng (2011) 44:531–540
DOI 10.1007/s00603-011-0157-2

ORIGINAL PAPER

In Situ Stresses in Borehole Blanche-1/South Australia Derived from Breakouts, Core Discing and Hydraulic Fracturing to 2 km Depth

G. Klee · A. Bunger · G. Meyer · F. Rummel · B. Shen

Received: 25 November 2009 / Accepted: 5 May 2011 / Published online: 19 May 2011

Abstract The development of Hot-Dry Rock (HDR) geothermal energy in Australia with drillings to some kilometres depth yields an impetus for deep stress logging. For the Olympic Dam HDR-project, borehole Blanche-1 was drilled to almost 2 km depth and provided the possibility to estimate the in situ stresses within the granitic borehole section by the analysis of borehole breakouts and core discing, as well as by hydraulic fracturing combined with acoustic borehole televiewer logging for fracture orientation determination. Although the stress magnitudes derived by the different methods deviate significantly, they clearly indicate for the depth range between 800 and 1,740 m a compressional stress regime of $S_v \leq S_h < S_H$ and a consistent East–West orientation of maximum horizontal compression in agreement with existing stress data for Australia. The minor horizontal stress S_h derived from the hydraulic fracturing closure pressure values is about equal to the overburden stress and may be regarded as most reliable.

Keywords Hot-Dry-Rock geothermal energy · Borehole breakouts · Core discing · Hydraulic fracturing · Stress data Australia

G. Klee (✉) · F. Rummel
MeSy-Solexperts GmbH, Meesmannstr. 49,
44807 Bochum, Germany
e-mail: gerd.klee@mesy-solexperts.com

A. Bunger
CSIRO Petroleum, Melbourne, Australia

G. Meyer
Green Rock Energy Ltd., West Perth, Australia

B. Shen
CSIRO Exploration and Mining, Brisbane, Australia

1 Introduction

Australia is strongly dependent on coal for electricity generation. In 2006, the electricity was produced from 51.4 GW_e capacity, of which 56% is coal fired, 18% hydro and 22% gas (http://www.world-nuclear.org 2009). However, the power generation contributes more than 30% of the country's net carbon dioxide-equivalent emission, making Australia's greenhouse gas emission per capita one of the highest in the world (43% above the IEA average). In this view, the Australian government announced in 1997 a number of substantial energy research, development and technology programmes, which focus on carbon capture and storage, energy efficiency and development of renewable energies, including geothermal energy.

The geothermal resources in Australia concentrate mainly in the Cooper Basin in Central Australia, extending over the north-eastern corner of South Australia and the south-western corner of Queensland and have potential to become a secure, emission-free, renewable base-load power for the future (Goldstein et al. 2007). Although at present geothermal energy plays only a marginal role in Australia's energy market with only one 80 kW net hydrothermal plant in operation in Birdsville, Queensland, the interest of private companies for exploring geothermal energy has increased significantly during the past decade. By the end of 2007, 29 companies had applied for geothermal licences, mainly focussing on the Hot-Dry-Rock (or Enhanced Geothermal System) concept, and five companies had started drilling at potential sites (http://www.ga.gov.au 2009): Habanero-project of Geodynamics Ltd., Paralama and Callabonna-projects of Petratherm, Lake Frome project of Geothermal Resources, the projects near Millicent and Beachport of Scopenergy Ltd., and the Olympic Dam-project of Green-Rock Energy Ltd.

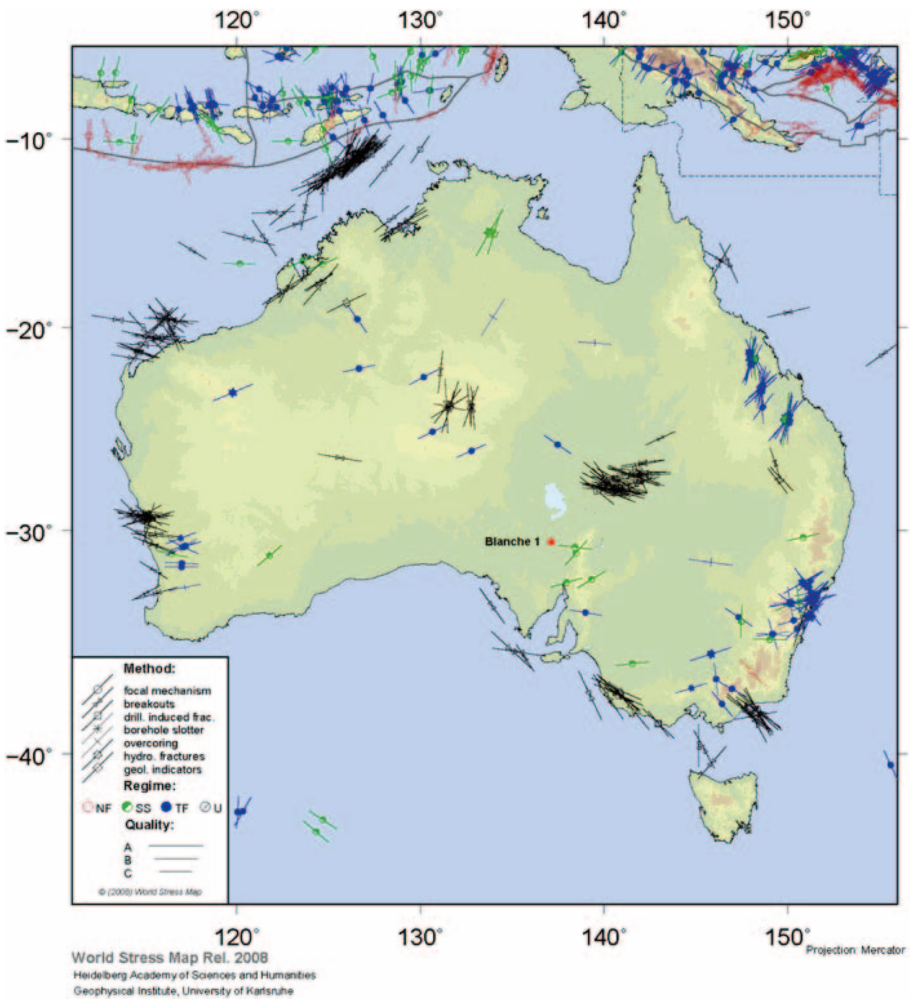

Fig. 1 Australian stress map and location of borehole Blanche-1 (after Heidbach et al. 2008)

The Hot-Dry-Rock (or EGS) concept is based on the assumption that deep crystalline rock formations are practically dry and impermeable due to the high pressure of the overburden layers. Therefore, it was proposed to induce artificial fractures as heat exchangers through which fluid (water) is forced to flow from an injection borehole to a production borehole (e.g. Rummel 2005). Development of the reservoir depends on hydraulic fracture stimulation, with the orientation of the newly created or reopened fractures determined by the in situ stress. Furthermore, the efficiency of the heat exchange by fluid circulation between deep boreholes strongly depends upon the hydraulic impedance of the fluid-flow path, which is mainly controlled by the in situ stress regime. Therefore, the determination of the in situ stresses is an important part of feasibility studies for the design of HDR-operation. The present paper summarizes the results of in situ stress estimations in the geothermal exploration borehole Blanche-1 of the Olympic Dam project, derived from borehole breakout- and core discing analysis and hydraulic fracturing to about 2 km depth.

2 Borehole Blanche-1: Geology and Tectonics

Borehole Blanche-1 (Fig. 1, S30°28.203′, W136°47.817′) is located about 550 km north of Adelaide in South Australia, close to the giant Olympic Dam copper—gold—silver and uranium mine, with the largest known single deposit of uranium in the world. The drill-site is situated near the western edge of the Roxby Downs Granite, which forms part of the Burgoyne Batholith. The Batholith contains a suite of moderately magnetic, radiogenic granitoids, which are part of the Olympic Domain of the Gawler Craton. The granitoids are generally mesoproterozoic in age and are considered as the source of the elevated heat flow up to 125 mW/m^2 in the area (Housemann et al. 1989).

Drilling of borehole Blanche-1 in 2005 to 1,934 m depth demonstrated granitic rocks below a cover sequence of sedimentary rocks with a mean density of 2.6 g/cm^3 to 718 m depth. The cover sequence comprises several insulating shale units with a combined thickness of 469 m, as well as sandstone- and limestone sequences. The granite

Table 1 Physical properties of the granite

Property	Number of cores tested	Mean value
Density ρ (g/cm^3)	13	2.634 ± 0.028
P-wave velocity v_p (km/s)	15	5.00 ± 0.56
S-wave velocity v_s (km/s)	15	2.91 ± 0.33
Young's modulus E_{dyn} (GPa)	15	56 ± 11
Young's modulus E_{stat} (GPa)	5	57 ± 17
Poisson's ratio v_{dyn}	15	0.24 ± 0.01
Poisson's ratio v_{stat}	5	0.29 ± 0.07
Fracture toughness K_{IC} (MPa m$^{1/2}$)	4	2.21 ± 0.86
Uniaxial compressive strength σ_c (MPa)	5	160 ± 54
Hydraulic tensile sample strength p_{co} (MPa)	5	25
Hydraulic in situ tensile strength P_{co} (MPa)	7	4.8 ± 1.2
In situ permeability *k* (μDarcy)	4	2.6 ± 1.5

consists of syenogranite and monzogranite. The granites are generally massive without large shear zones, but with several zones of low- and high-angle inclined fractures. Below 1,034 m depth, extensive core discing was observed. Within the granitic section of the borehole, the geothermal gradient is about 30°C/km and the thermal conductivity is 3.2 W/mK. The physical properties of the granite measured on the core material and used in the stress analysis are given as mean values in Table 1.

The Australian stress map (Fig. 1) clearly shows a significant scatter in the orientation of the maximum horizontal stress, particularly in comparison with other intraplate regions like Western Europe, North America or South America. Nevertheless, a number of stress provinces with broadly consistent stress orientations were defined by Reynolds et al. (2002), with a predominant WNW–ESE to E–W orientation of the maximum horizontal stress in the Cooper Basin, about 500 km north-east of borehole Blanche-1. Deviating from this trend, the analysis of borehole breakouts and drilling-induced fractures observed in several exploration boreholes at the Olympic Dam mine at depths between 400 and 600 m suggest a NW–SE orientation of the maximum horizontal stress (Fowler and Weir 2007). Leak-off tests in petroleum wells in the Cooper Basin down to about 3 km depth indicate a ratio between the minimum horizontal stress and the vertical stress of about 0.65–0.85 (Nelson et al. 2007).

3 Stress Estimates in Borehole Blanche-1

3.1 Analysis of Borehole Breakouts

Breakouts are zones of failure of the borehole wall as a result of high compressive stress concentration around the wellbore (e.g. Bell and Gough 1979). In borehole Blanche-1, pronounced breakouts and regular ovalisations of the borehole were identified in the borehole televiewer logs below 1,146 m depth. In all cases, the breakout direction is consistently North–South, indicating an East–West orientation of the maximum horizontal stress.

While borehole breakouts are reliable indicators of the horizontal stress direction, the determination of the stress magnitudes from the breakout geometry has to be considered with caution since the width and depth of breakouts are influenced by several factors such as rock strength, borehole diameter, temperature and chemical effects, or drilling methodology (Amadei and Stephansson 1997). Despite these limitations, a study was conducted using the two-dimensional boundary-element code FRACOD (Shen et al. 2004) which enables to simulate the rock fracture initiation and propagation during breakout formation. Considering the deep vertical borehole and the long and consistent breakout sections, the 2D approach is adequate. The input parameters were based on drilling operational data and a mean laboratory uniaxial compressive strength of 120 MPa. For three cross-sections at 1,146.5, 1,247.5 and 1,392.5 m depth, the measured breakout dimensions were modelled for different in situ stress ratios of $S_h/S_v = 0.75$–2 and $S_H/S_V = 2.5$–3 (S_h minimum horizontal stress, S_H maximum horizontal stress, S_v vertical stress) until a satisfactory agreement with the measured breakout geometry was achieved. An example for the analysis of the breakout cross-section at 1,392.5 m depth is shown in Fig. 2. The best-fit result suggests in situ stress-ratios of $S_H/S_h/S_v = (2.5$–$2.75)/(1.25$–$1.5)/1$.

3.2 Analysis of Core Discing

Core discing occurs due to drilling-induced tensile stress within or below a core stub (Kaya et al. 2003). Extensive core discing was observed in borehole Blanche-1 below

Fig. 2 Measured (*top*) and predicted (*bottom*) breakout geometry at 1,392.5 m for $S_H/S_h/S_v = 2.75/1.25/1.0$

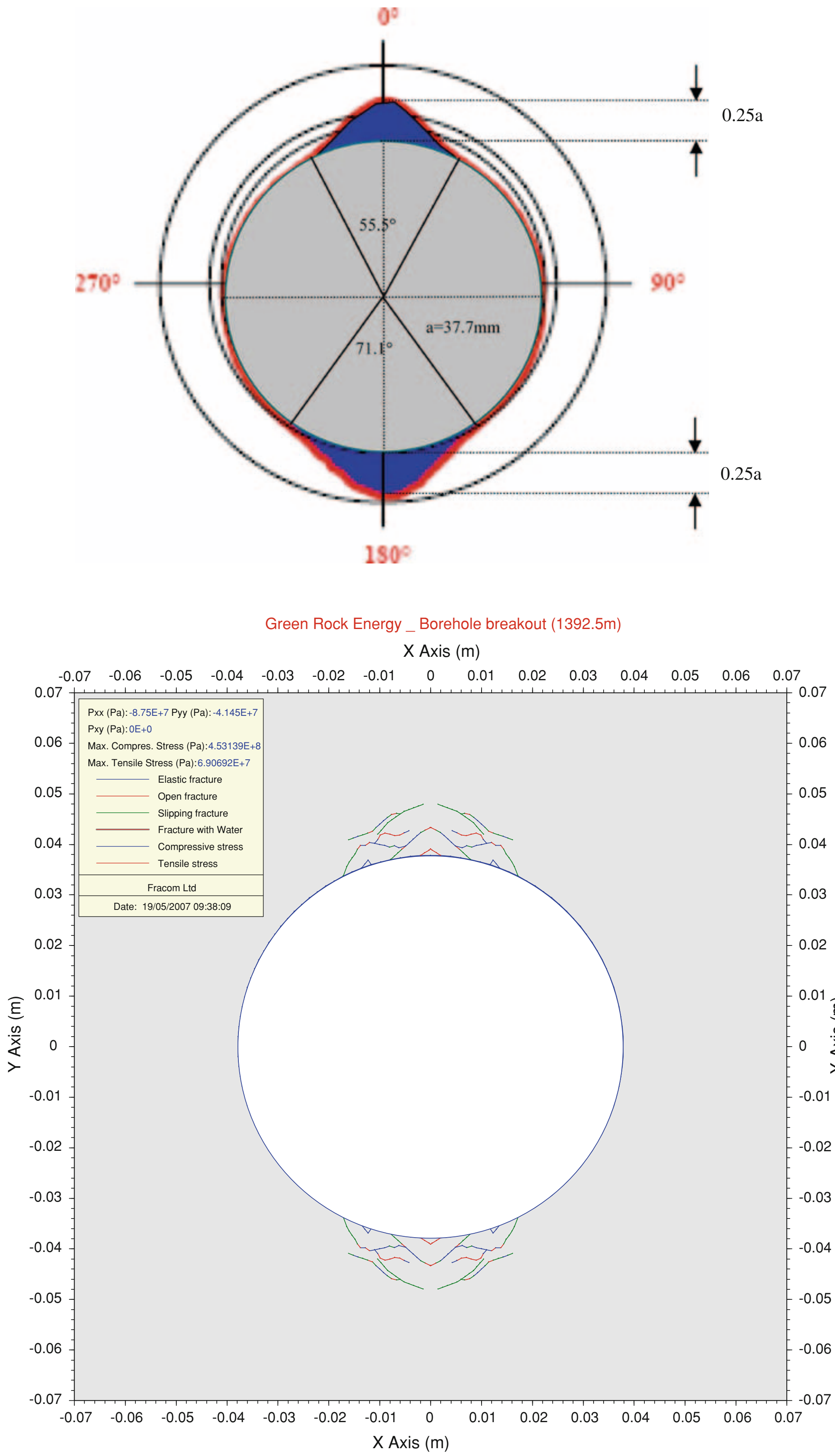

Fig. 3 Example of saddle-shaped discing/fragmentation near 1,422.5 m depth (after Bunger 2010)

1,034 m depth (Fig. 3). The discs are relatively flat, slightly upwardly cup-shaped, or saddle-shaped. In some cases a core section containing saddle-shaped discs were re-oriented using inclined fractures that could be matched to the borehole televiewer logs. The corresponding direction of the maximum upward curvature of the saddle-shape, which is expected to align with the direction of the minimum horizontal stress (e.g. Matsuki et al. 2004) is oriented N(185–187)°. This stress direction is in agreement with the stress direction derived from the breakout analysis, and gives strong support to the basic notion of core discing analysis, that the disc geometry is primarily controlled by in situ stresses.

The magnitude of the in situ stresses was inferred by studying the length of the core discs using a novel, and therefore hitherto relatively unproven, stochastic analysis method. Details of the analysis are presented by Bunger (2010). Eight zones ranging from 40 to 70 m were chosen for examination. In total, the length of nearly 5,500 discs was measured and histograms of the disc length were constructed for each of the eight zones. Figure 4 shows two of the histograms, where N is the number of discs in a given histogram bin and L/R is the disc length/disc radius ratio. The histograms are presented along with graphical presentations of the discing showing the tendency of the shortest discs to be clustered together. Also, in both zones shown in Fig. 4, the mode of the distribution implied by the histogram is near $L/R = 0.5$. However, for the shallower case (1,029–1,079 m), most of the discs are in the right tail of the distribution, i.e. $L/R > 0.5$; for the deeper case (1,887–1,926 m) the disc lengths are more evenly distributed between the left and right tails in the manner of a classical bell-shaped or Gaussian distribution. As such, a transition is observed from strongly right-tail dominated to bell-shape distributions as the depth increases.

The complex distribution implies that a typical length of discs is not well defined, except for the deepest of the eight zones, because of the right-tail dominance of the distributions. Hence, existing approaches to core discing analysis

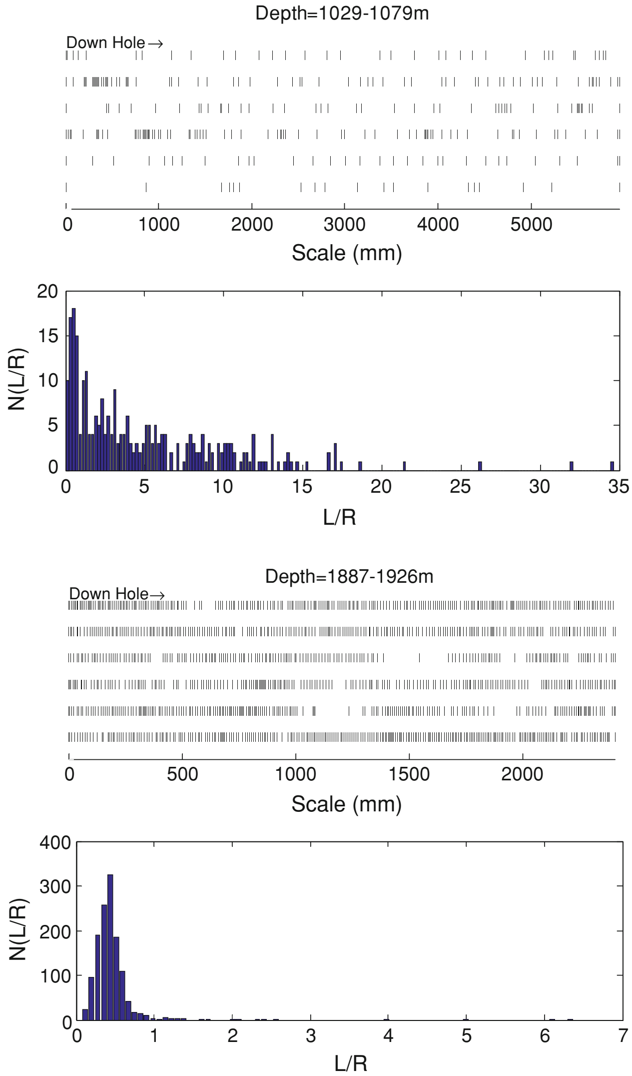

Fig. 4 Right-tail dominant (*top*) and bell-shape (*bottom*) core disc length distributions observed between 1,029–1,079 m and 1,887–1,926 m depth (Bunger 2010)

are not applicable and a stochastic approach has been proposed with the following premises:

- The observed disc length distributions are caused by unknown statistical variations in the in situ stresses and rock tensile strength;
- The core will break off to form a disc of a certain length if the local stress and rock strength conditions satisfy a mechanically determined failure criterion (Matsuki et al. 2004):

$$\sigma_x k_x\left(\frac{L_s}{R}\right) + \sigma_y k_y\left(\frac{L_s}{R}\right) + \sigma_z k_z\left(\frac{L_s}{R}\right) - \sigma_t \geq 0 \qquad (1)$$

where, σ_x, σ_y, σ_z are the in situ stresses, k_x, k_y, k_z are numerically determined length-dependent functions and σ_t is the rock tensile strength;

Table 2 Results of core discing stress analysis

Average depth (m)	S_h (MPa)	S_H (MPa)	S_v (ρ = 2.65 g/cm^3) (MPa)
1,054.0	42.1	47.3	27.4
1,255.0	61.4	66.9	32.6
1,345.5	63.0	73.1	35.0
1,472.5	67.8	78.6	38.3
1,569.0	71.0	81.8	40.8
1,673.0	72.6	90.7	43.5
1,779.0	76.3	88.5	46.3
1,906.5	79.7	80.5	49.6

- The probability of forming a disc with a given length is the probability of discing at that length and not discing at a shorter length.

Then, by assuming that the in situ stresses and the rock tensile strength follow normal distributions, a Monte Carlo technique was used to predict disc length distributions for given in situ conditions until the predicted histograms match the measured data as closely as possible. The resulting in situ horizontal stresses S_h and S_H are summarized in Table 2 together with the vertical stress S_v calculated for a mean overburden rock mass density of 2.65 g/cm^3. While the maximum horizontal stress is about twice of the vertical stress (except for the sections at 1,054 and 1,906.5 m), the analysis yields rather high minimum horizontal stresses with a ratio of $S_h/S_H \approx 0.9$.

3.3 Hydraulic-Fracturing Stress Measurements

The hydraulic fracturing tests in borehole Blanche-1 were carried out by using a wireline hydrofrac system, described in detail by Rummel (2002). The technique allows fast 'stress-logging' in the absence of an on-site drill-rig. Furthermore, compared with conventional systems with drill-rods, the wireline approach has the advantage of a high hydraulic system stiffness, which enables detailed fracture growth control and the possibility of online downhole high-resolution pressure recording. A schematic view and a photo of the system with all its main components are shown in Fig. 5.

In the case of the hydraulic fracturing experiments in the 76 mm diameter borehole Blanche-1, a straddle packer assembly with Kevlar-reinforced packer elements of 40 MPa pressure capacity (OD: 71 mm) was used. The tool is moved within a borehole on a seven-conductor logging cable with a mobile winch. The packers and the injection interval are pressurized via a stainless steel coil tubing which is clamped to the wireline cable. A mechanically operated push–pull valve on top of the packer assembly permits to switch from packer pressurization to injection

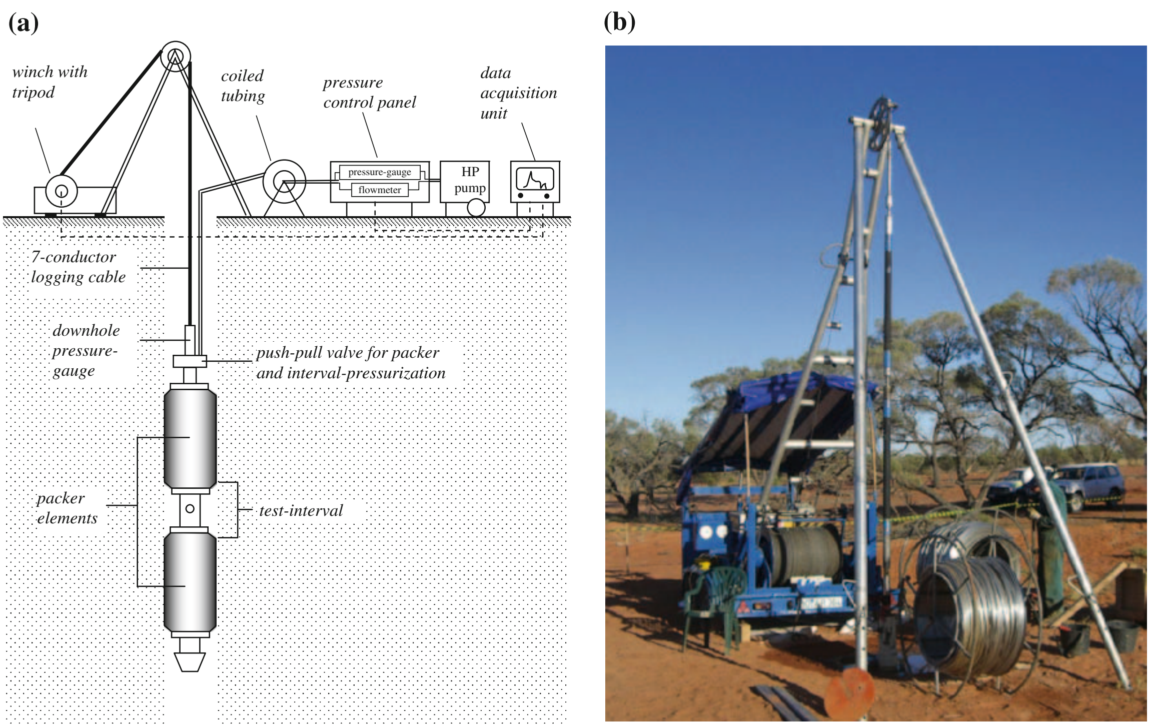

Fig. 5 **a** Schematic view of the wireline hydrofrac system, **b** photo showing essential details of the wireline hydrofrac system (winch incl. tripod, straddle packer tool, coil-tubing drums)

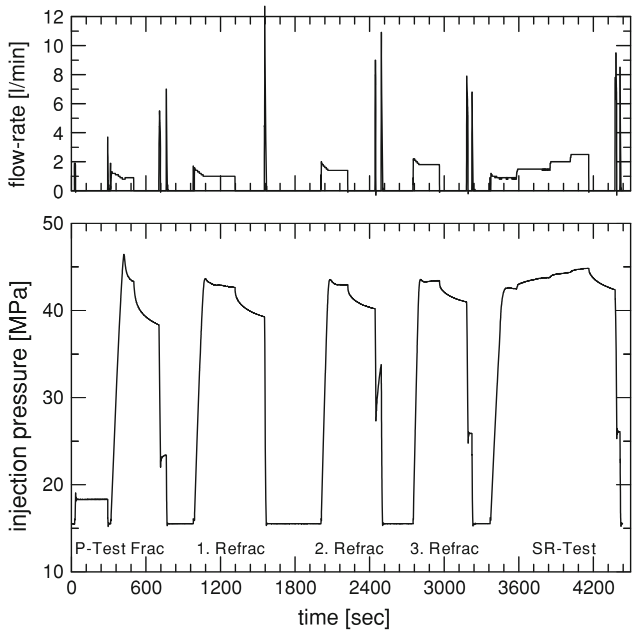

Fig. 6 Downhole injection pressure and surface flow-rate record of the hydraulic fracturing test at 1,534.8 m depth in borehole Blanche-1

Table 3 Results of hydraulic fracturing tests in borehole Blanche-1

Depth (m)	P_c (MPa)	P_r (MPa)	P_{si} (MPa)	θ (°)	α (°)
881.1	25.55	20.1	18.9	68	85
952.5	22.8	19.2	17.5	89	84
1,052.1	34.65	31.2–31.8	26.3	98	40
1,110.9	27.6	22.1	21.6	88	82
1,212.0	39.9	36.1	31.9	112	31
1,286.9	–[a]	19.0–21.6	23.4	98	89
1,370.5	–[a]	32.4	31.1	60	4
1,456.2	–[a]	41.8	42.2	125	65
1,534.8	46.4	40.8	42.2	122	81
1,541.5	48.3–49.1	42.5	43.5	111	11
1,599.6	>52.1				
1,618.7	–[a]	47.6	50.4	95	5
1,738.5	–[a]	44.0	46.9	101	79

P_c breakdown pressure, P_r refrac pressure, P_{si} shut-in pressure, θ fracture strike direction counted N over E, α dip of fracture with respect to horizontal

[a] Stimulation of pre-existing fractures

into the 0.7 m long test interval. Hydraulic pressure is generated by a frequency-controlled electric-driven three plunger pump with a maximum working pressure of 40 MPa and a maximum injection rate of 10 l/min. The measuring and recording system consists of appropriate pressure transducers downhole and on surface, a surface flow-meter, and a digital data acquisition system (16 bit resolution, 5 Hz sampling rate). The orientations of induced or stimulated fractures were determined by acoustic televiewer logging after hydraulic fracturing testing.

The test conduction closely followed the recommendations of both, the ISRM standard (2003) and the ASTM D4645 (1997). A typical test record to illustrate the test procedure is shown in Fig. 6 for the test at 1,534.8 m depth. Prior to fracturing the permeability of the rock mass is measured by rapidly pressurizing the test interval to about 2 MPa and observing the subsequent pressure decline in the hydraulically closed system. After complete venting of the test interval, the pressure is increased again until either a sudden pressure drop related to the initiation of a fracture in the borehole wall (frac cycle) or to the stimulation of an existing fracture. In both cases, the initiated or stimulated fractures are extended during several subsequent pressure cycles (refrac cycles) and a final step-rate injection cycle. During each test, a total volume of 20–50 l of water was injected which was partly recovered during depressurizations depending on whether the induced or stimulated fracture remains isolated or intersects an open joint system. Such tests were repeated at different depth sections to derive a stress-depth profile.

Because the accuracy of hydraulic fracturing stress measurements strongly depends on the correct interpretation of the pressure–time records obtained during the tests, the characteristic hydrofrac pressure values breakdown pressure P_c, refrac- or re-opening pressure P_r, and shut-in pressure P_{si} were identified using various graphical procedures discussed by Baumgärtner and Zoback (1989). The results of the analysis together with the orientation of induced or stimulated fractures are summarized in Table 3. In seven of the 13 tests, fracture initiation events with breakdown pressure values between 22.8 and 49.1 MPa were observed; in five test sections pre-existing fractures were stimulated without distinct pressure peaks. No fracture could be initiated at 1,599.6 m depth due to the pressure limitations of the packer tool. The refrac-pressure values increase from 19.2 to 47.6 MPa, and the shut-in pressure values range between 17.5 and 50.4 MPa. The post-frac BHTV-log shows that mainly E–W striking fractures, either steeply inclined or sub-horizontal, were initiated or stimulated.

The calculation of the in situ principal stresses was based on two independent methods. First, in the case where vertical to sub-vertical fractures with similar orientation were initiated or stimulated, the Hubbert and Willis (1957) equation for the critical pressure P_c for fracture initiation in a vertical borehole was applied:

$$P_c = 3 \cdot S_h - S_H + P_{co} - P_o \tag{2}$$

where S_h and S_H are the horizontal far-field principal stresses, P_{co} is the in situ hydraulic tensile strength of the rock and P_o is the pore pressure in the rock mass. It is assumed that the vertical stress is a principal stress and equal to the overburden stress, the rock is homogeneous, isotropic and initially impermeable (no fluid penetration into the rock prior to fracture initiation) and that the induced fracture is oriented perpendicular to the minimum horizontal principal stress S_h. The last assumption yields.

$$S_h = P_{si} \tag{3}$$

where P_{si} is the shut-in pressure to keep the fracture open after the hydraulic injection is interrupted and the pressurizing system is shut-in. Neglecting the pore pressure P_o in low-permeable crystalline rock, the principal stresses can be expressed by the relations:

$$\begin{aligned} S_h &= P_{si} \\ S_H &= 3 \cdot P_{si} - P_r \\ S_v &= \rho \cdot g \cdot z \end{aligned} \tag{4}$$

where $P_r = P_c - P_{co}$ is the pressure to re-open an induced fracture during subsequent pressurization cycles. The assumption that for a flat-lying region the vertical stress S_v is equal to the weight of the overburden rock with density ρ is a matter of pure static's and force equilibrium (Jaeger and Cook 1969) and is confirmed by numerous measurements.

Second, in order to incorporate the pressure and fracture orientation data of tests on arbitrary oriented fractures, an inversion type stress analysis introduced by Cornet and Valette (1984) or Baumgärtner and Rummel (1989) was conducted. The method is based on the shut-in pressure P_{si} as a measure of the normal stress S_n acting across the fracture plane considered:

$$S_n = P_{si} \tag{5}$$

Assuming that the vertical stress S_v is a principal stress and the stress field linearly varies with depth, the normal stress $S_{n,i}$ is

$$\begin{aligned} S_{n,i} = {} & S_v \cdot \cos^2\alpha + \frac{1}{2}\sin^2\alpha\{[S_{Ho} + S_{ho} + (dS_H/dz + dS_h/dz) \cdot z_i] \\ & -[S_{Ho} + S_{ho} + (dS_H/dz + dS_h/dz) \cdot z] \cdot \cos 2(\theta - \theta^*)\} \end{aligned} \tag{6}$$

where θ and α are the strike and dip angles of the particular fracture plane at depth z_i, S_{Ho} and S_{ho} are the principal horizontal stresses at the upper limit of the investigated borehole section, the stress derivatives are the horizontal principal stress gradients and θ^* is the orientation of S_{Ho} with respect to north. The equation includes six unknowns; the solution therefore requires a minimum of six measurements of S_n at various depths on fractures with different orientation. The method is attractive since shut-in pressures are easy to identify and are usually reliable. In addition, no assumptions on the pore pressure are required.

Using eleven of the 12 data sets (the test at 1,618.7 m depth was neglected due to the inconsistency of the high shut-in pressure of about 50 MPa and the observed horizontal fracture), the calculated principle in situ stresses are summarized by the following linear stress-depth relations within the depth range tested between 880 and 1,740 m:

$$S_h = (12.4 \pm 1.2) + (0.038 \pm 0.003) \cdot (z - 880)$$
$$S_H = (35.8 \pm 2.8) + (0.060 \pm 0.010) \cdot (z - 880)$$

The vertical principal stress S_v was calculated for an average rock mass density of 2.65 g/cm^3:

$$S_v = 0.026 \cdot z$$

where z is the depth in metres, and S_h, S_H, S_v are the principal stresses in MPa.

The hydraulic fracturing tests yield a direction of the maximum horizontal principal stress S_H of N(97 ± 3)° (approx. E–W), in close agreement with both, the stress direction derived from the analysis of breakouts (E–W) and core discing (N 95–97°).

The stress magnitudes derived from the hydraulic fracturing tests are shown in Fig. 7 together with the results of the borehole breakout and core discing analysis. It is realized that the minor principal stress S_h is clearly less than the vertical stress S_v above 1,320 m depth and exceeds the vertical stress at greater depth. This is in contradiction with the results from leak-off tests conducted in petroleum wells in the Cooper Basin which show a minor horizontal stress S_h ranging between 65 and 85% of the vertical stress S_v to a depth of 3 km (Nelson et al. 2007). The major horizontal stress S_H is about twice the minor horizontal stress.

It should be mentioned that a comprehensive laboratory study was conducted on the core material of borehole Blanche-1 for the determination of hydrofrac-related physical rock properties (elasticity, permeability, fracture toughness, hydrofrac tests on mini-cores subjected to confining pressure). These data (Table 1) were used for fracture mechanics simulation calculations to match the in situ measured frac-cycle records as quality control.

4 Discussion and Conclusions

The analysis of borehole breakouts, core discing and hydraulic fracturing tests in borehole Blanche-1 yield consistently an East–West orientation of the maximum horizontal principal stress S_H. Although this direction is in agreement with existing stress data for the Cooper Basin about 500 km north-east of the test site (Reynolds et al. 2002), the direction deviates from the stress orientation in the nearby Olympic Dam mine, where a S_H-direction of

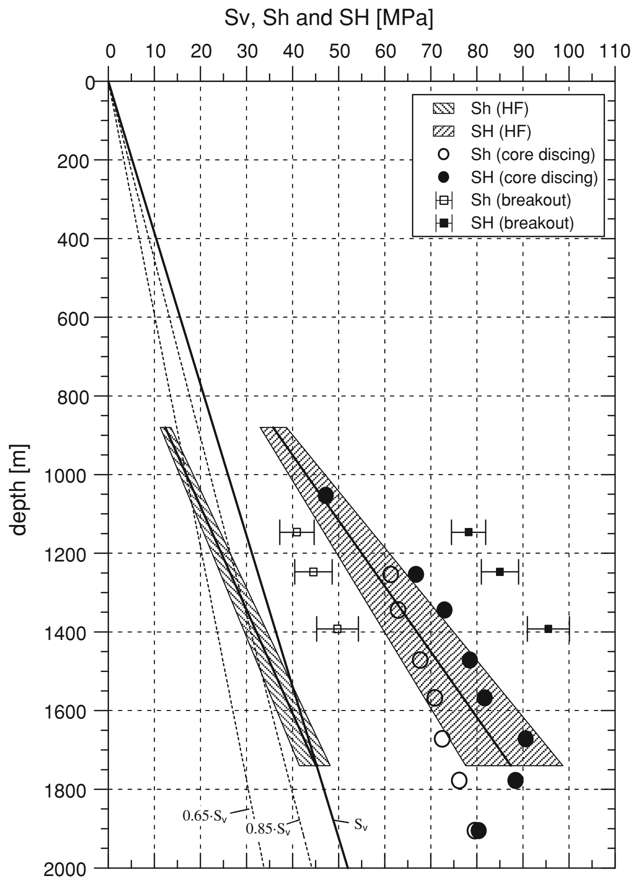

Fig. 7 Comparison of stress data for borehole Blanche-1 as derived from hydraulic fracturing, analysis of core discing, and borehole breakouts. The *shaded zones* with *solid lines* represent the stress-profiles and range of uncertainty of the hydraulic fracturing stress analysis

NW–SE is dominantly observed (Fowler and Weir 2007). However, the in-mine stress direction is likely influenced by the existence of local faults within the ore body and the mine openings itself.

Both the analysis of core discing and borehole breakouts observed in borehole Blanche-1 suggests rather high horizontal stresses with $S_h \approx S_H > S_v$ and $S_H > S_h > S_v$, respectively. Both methods are using rock strength data which, however, are strongly dependent on the granite conditions at the specific depth sections and are representing the stress field over smaller rock volumes rather than the hydraulic fracturing method.

In comparison, the hydraulic fracturing tests in borehole Blanche-1 carried out at depth between 880 and 1,740 m clearly demonstrate that the induced or stimulated fractures open for substantial water flow at pressures below or about equal to the overburden stress S_v. Since most of the induced or stimulated fractures were nearly vertical, this means that the horizontal normal stresses acting across these fractures must be in the order of magnitude of or slightly less than S_v, which can be estimated from the mean density of the overburden or from the shut-in pressure values of the hydraulic fracturing tests on sub-horizontal fractures. Thus, the magnitude of S_h derived from the hydraulic fracturing tests must be considered as realistic for the basement rock to a depth of 1,740 m. Similarly, both, leak-off tests and mini-frac tests carried out in boreholes within the Cooper Basin indicate minor horizontal stresses with gradient of 14–25 MPa/km, i.e. $S_h \leq S_v$ (Nelson et al. 2007). Furthermore, the calculation of the maximum horizontal stress S_H by the inversion method considering the scatter of fracture orientations as shown in the acoustic televiewer logs only depend on the reliable shut-in pressure data. Therefore, the derived stress profiles for S_h and S_H for the investigated depth range must be considered as realistic.

Some further specific aspects of the stress estimation by the different methods are:

- The analysis of borehole breakouts yield the highest horizontal principal stresses, most likely due to uncertain assumption on rock strength.
- A reasonable agreement exists for the maximum horizontal principal stress S_H derived from the core discing analysis and the hydraulic fracturing results. An exception is the trend of the stresses below 1,700 m, with the core discing indicating S_H decreasing from 1,700 to 1,900 m. While this could indicate a changing stress regime, it is more likely that the core discing estimate becomes less reliable for two reasons. First, the core is reduced to rubble over many sections below 1,700 m, enforcing that many thin discs, which would tend to drive higher estimated of S_H are not present in the data set. Additionally, the mechanical model of Matsuki et al. (2004) used for the core discing analysis is an elastic model and therefore it neglects post failure behaviour of the rock. Hence, the model may become less appropriate as the stress increases below 1,700 m. Nonetheless, the comparison with the authors' knowledge is the most promising approach that has been presented to date and the utility of core discing analysis can only be expected to increase as the basic assumptions are addressed by further research.
- The core discing analysis yields the highest estimation of the minimum horizontal principal stresses S_h. The most likely cause of the mismatch is that the core discing analysis relies on a detailed analysis of the stresses near the base of an advancing core barrel that is specified in the used model for an HQ-size borehole geometry (Matsuki et al. 2004), while borehole Blanche-1 was drilled with an NQ2 core-barrel. Other possibilities include that the spatial orientation among the in situ quantities is neglected in the discing analysis. Finally, the analysis presented here neglects the fact that the fracturing which forms the core disc is not

expected to correspond exactly to the base of the core barrel.

- The results of the different stress determination methods indicate that the vertical principal stress S_v is the minimum principal stress, at least at the bottom of the investigated borehole section. Linear extrapolation of the stress-profiles to the proposed geothermal reservoir depth of 4–5 km yields a stress regime with high horizontal stresses, which will favour the creation of horizontal fractures during future massive stimulation operations for permeability enhancement and will require operating pressure in the order of the vertical stress. While this conjecture admittedly relies on extrapolation, it is assumed that the granite below 718 m depth continues as a relatively homogeneous massive body to well below 5 km depth, and therefore the extrapolation to greater depth may be reasonable. The stress conditions at depth, therefore, significantly contribute to economic considerations for the development of HDR geothermal energy in South-Australia.

Acknowledgments The authors wish to acknowledge the kind approval of GreenRock Energy Ltd., West Perth, to publish the results of the stress investigations in borehole Blanche-1. The work presented was conducted by CSIRO, Melbourne, and MeSy GmbH, Bochum, in close cooperation with GreenRock Energy Ltd. The excellent collaboration of all participants is appreciated. The authors wish to thank Dr. Rob Jeffrey (CSIRO Melbourne) for his constructive comments on an early version of this manuscript.

References

Amadei B, Stephansson O (1997) Rock Stress and its Measurement. Chapman & Hall, London

ASTM D4645 (1997) Standard Test Method for Determination of In Situ Stress in Rock using the Hydraulic Fracturing Method. American Society for Testing and Materials

Baumgärtner J, Rummel F (1989) Experience with "fracture pressurization tests" as a stress measuring technique in a jointed rock Mass. Int J Rock Mech Min Sci Geomech Abstr 26–6:661–671

Baumgärtner J, Zoback MD (1989) Interpretation of hydraulic fracturing pressure-time records using interactive analysis methods. Int J Rock Mech Min Sci Geomech Abstr 6:461–470

Bell JS, Gough DI (1979) Northeast-southwest compressive stress in Alberta: evidence from oil wells. Earth Planet Sci Lett 45:475–482

Bunger AP (2010) Stochastic analysis of core discing for estimation of in situ stress. Rock Mech Rock Eng 43:275–286

Cornet FH, Valette B (1984) In situ stress determination from hydraulic injection test data. J Geophys Res 89:11527–11537

Fowler MJ, Weir FM (2007) The use of borehole breakouts for geotechnical investigation of an open pit mine. Proc. of the 1st SHIRMS 2007, Perth, Australia. Potvin Y, Carter J, Dyskin A, Jeffrey R (eds) Australian Centre of Geomechanics

Goldstein B, Hill AJ, Budd AR, Malavazos M (2007) Hot rocks in Australia—national outlook. Proc. of 1st European geothermal review, geothermal energy for electricity power production. Mainz, Germany

Heidbach O, Tingay M, Barth A, Reinecker J, Kurfeß D, Müller B (2008) The world stress map database release 2008. doi:10.1594/GFZ.WSM.Rel2008

Housemann GA, Cull JP, Muir PM, Paterson HL (1989) Geothermal signatures and uranium ore desposits on the stuart shelf of South Australia. Geophysics 54(2):158–170

Hubbert MK, Willis DK (1957) Mechanics of hydraulic fracturing. Trans AIME 210:153–163

ISRM Standard (2003) Suggested methods for rock stress estimation—Pt. 3: hydraulic fracturing (HF) and/or hydraulic testing of pre-existing fractures (HTPF). Int J Rock Mech 40:1011–1020 (authors: BC Haimson, FH Cornet)

Jaeger JC, Cook NGW (1969) Fundamentals of rock mechanics. Chapman and Hall, London

Kaya N, Matsuki K, Sakaguchi K (2003) The in situ stress state associated with core discing estimated by analysis of principal tensile stress. Int J Rock Mech Min Sci 40(5):653–665

Matsuki K, Kaya N, Yokohama Y, Tsuda T (2004) Determination of three-dimensional in situ stress from core discing based on analysis of principal tensile stress. Int J Rock Mech Min Sci 41:1167–1190

Nelson JN, Chipperfield ST, Hillis RR, Gilbert J, McGrowen J, Mildren SD (2007) The relationship between closure pressure from fluid injection tests and the minimum principal stress in strong rocks. Int J Rock Mech Min Sci 44:787–801

Reynolds SD, Coblentz DD, Hillis RR (2002) Tectonic forces controlling the regional intraplate stress field in continental Australia: results from new finite element modelling. J Geophys Res 107(B7):2131. doi:10.1029/2001JB000408

Rummel F (2002) Crustal stress derived from fluid injection tests in boreholes. In: Sharma VM, Saxena KR (eds) In situ characterization of rocks. A.A. Balkema Publisher, pp 205–244

Rummel F (2005) Geothermal energy—an energy option for the future. In: Rummel F (ed) Rock mechanics with emphasis on stress. A.A. Balkema Publisher, pp 151–168

Shen B, Stephansson O, Rinne M, Lee H-S, Kobayashi A (2004) FRACOD for continuum, discontinuum and fracture modelling of rocks. Schubert (ed) Proc. of EUROCK 2004 and 53rd Geomechanics Colloquium, Salzburg. pp 707–712